by Paolo Vallerotonda[1,2], Fabrizio Cacciamani[1], Luca Pelliccia[1], Francesco Aquino[1], Cristiano Tomassoni[2], Vittorio Tornielli di Crestvolant[3]
1. RF Microtech - 2. University of Perugia - 3. ESA ESTEC

Ku-band filter design for high power space applications using Ansys simulators

This paper presents the design and first experimental results of a very compact Ku-band bandpass filter for high power satellite applications. The filter was designed and simulated using the Ansys HFSS and Mechanical simulators. Proposed as part of an ESA ARTES Advanced Technology project, the filter is based on dielectric loaded combline resonators. Several dielectric materials were considered and two models of the same filter are presented in this paper. The geometries and materials were chosen to improve the performance in terms of power-handling and multipactor up to 150 W continuous wave of input RF power. Barrel-shaped metal cavities and high-permittivity ceramic materials were mixed to minimize volume occupancy while maintaining high unloaded Q-factor values (>4500).

This paper proposes the design of a Ku-band filter based on dielectric loaded combline resonators for high power space applications. The requirements of the ESA ARTES AT project, named DOMUK (Dielectric-loaded high-power Output de-MUltiplexer at Ku/Ka-band, ESA Contract Number: 4000125645/19/NL/NR) were considered as a benchmark. In this scenario, output De-Multiplexers (ODEMUXs) are used in current multi-beam Ku/Ka systems to separate the signals intended for each beam. A large number of identical ODEMUXs are required in multi-beam systems due to the nature of the frequency re-use scheme. This implies very stringent requirements for the ODEMUX in terms of mass and footprint. There are numerous solutions in the literature to achieve more compact and lightweight filter structures without compromise the radio frequency (RF) performance. A general description of the techniques and technologies related to filter development is presented in [1]-[3]. Dielectric resonators

(DRs) are the preferred solution to minimize volume occupancy by high-permittivity (ε_r) materials. This solution is widely used for Input Multiplexer (IMUX) channels in all bands, and for high power Output Multiplexer (OMUX) channels in C-band. However, this approach is limited to moderate power levels per channel when considering K-band OMUXs with narrow bandwidth. The design of a high-power Ku-band filter is described in this paper where the architectures and materials have been carefully chosen to improve the performance of the filter with respect to power handling and multipactor up to 150 W of input RF power.

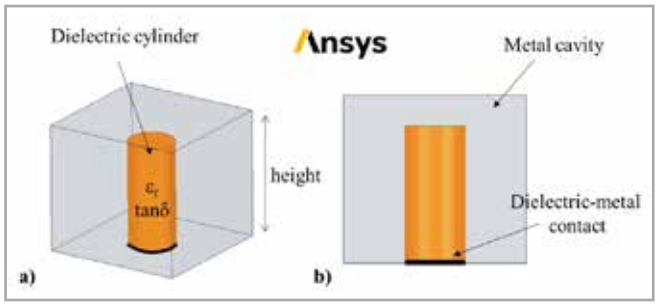

Fig. 1 - Dielectric loaded combline resonator designed in Ansys HFSS: a) 3D view, b) side view.

Several promising solutions could be adopted for our purpose; TM_{010} or $TE_{01\delta}$ dielectric resonator mode-based filters are an example. $TE_{01\delta}$ modes could represent the best compromise to obtain compact filters where low losses and high discharge handling capability are required. On the other hand, the main drawback of this solution concerns the thermal management [4] since the DR is not directly joined to the metal cavity of the filter, but is supported by a material with low dielectric permittivity generally characterized by a very poor thermal conductivity. With respect to the TM_{010} mode solution, the main limitation concerns the mechanical stability of the dielectric-metal contact [5]. In fact, the different Coefficients of Thermal Expansion (CTE) of the metal cavity and the ceramic element can produce detachment at the interfaces of the two materials when the operating temperature changes. Any small airgaps are sufficient to worsen the filter response as the boundary conditions change. In this scenario, dielectric combline resonators [6] would likely be a good compromise to minimize the critical aspects that could be encountered using the TM_{010} or $TE_{01\delta}$ approaches.

The design of a high-power sixth-order pseudo-elliptic filter based on dielectric combline resonators is proposed in this paper. Preliminary results are also described in [7] and [8], however this paper shows updates in which two similar filter models are proposed using different permittivity values of the dielectric elements. The 3D filter models were designed using the Ansys software suite, in particular HFSS was used for electromagnetic design while Ansys Mechanical was chosen to simulate the mechanical/thermal performance. Details of the software configuration and the results achieved are also presented in the paper, along with the preliminary test results.

Filter Design

The basic 3D model of the dielectric loaded combline resonators designed using Ansys HFSS software is shown in Fig. 1. The metal cavity is loaded by the dielectric cylinder with high permittivity values in order to increase the volume and mass saving (more than 50%) compared to standard TE113 resonators. The dielectric element is only joined to one side of the cavity, as shown in Fig. 1b.

Two sixth-order filter models were designed considering the different permittivity values of commercially available dielectric elements. The proposed resonator model for the filters is presented in Fig. 2; the high permittivity dielectric element is mixed with "barrel-shaped" metal cavity. Fig. 2a shows the combline resonator, which is based on ceramic material characterized by a permittivity of 12.6 and low loss-tangent (8e-5). This solution allows for a very compact structure while maintaining high unloaded Q-factor values (>4500) when considering a standard square cavity.

According to [7] and [8], along with the cavity height, the shape of the cavity can also be optimized to improve the Q-factor. It is well-known that a spherical shaped cavity is the best solution to maximize the Q-factor, however this approach could become critical to achieve the required coupling values for our filter since it increases the distance between two adjacent resonators.

Based on preliminary eigenmode analyses [7] performed in HFSS, the best cavity shape to further improve the Q-factor is the "Barrel" which allows the simulated unloaded Q-factor of the resonator in Fig. 2a to be increased up to 6000. In [7], [8] multiple parametric analyses were performed in HFSS with respect to the variation of the main parameters such as the radius of dielectric cylinder, cavity height, and curvature of the barrel cavity. As a result, (see Fig. 2a), the required aspect ratio of the ceramic cylinder to maximize the unloaded Q-factor is very high but a potentially vibration-sensitive structure is obtained. Therefore, support mechanisms (Teflon cups) were used to lock the ceramic cylinder in place on the top of the cavity. Along with the properties of the dielectric elements, the non-ideal characteristics of metallic material are also considered. The finite conductivity background conditions used in the models shown in Fig. 2a and Fig. 2b are set in order to consider the loss contribution due to the metal casing, as shown in Fig. 2c. Aluminum's similar bulk conductivity (σ=3e7 S/m) was also considered despite a silvering process having been performed on the cavity surfaces, which allows for a margin over than the desired true Q-factor.

In Fig. 2, the first prototype resonator (Fig. 2a) is compared with a smaller barrel-shaped resonator (Fig. 2b) in which a ceramic material with higher permittivity is used. Due to ε_r=24, additional shrinkage of the structure is achieved while maintaining a sufficiently high unloaded Q-factor value (about 4000-5000). The barrel shape of the cavity is less pronounced in the second resonator solution. To increase the "barrel-shape" to be similar to the first prototype, the diameter of the ceramic cylinder must be decreased. However, in this case, a minimum diameter of 2 mm was chosen to avoid possible criticality due to the robustness of the ceramic parts; for this reason a less pronounced barrel was obtained.

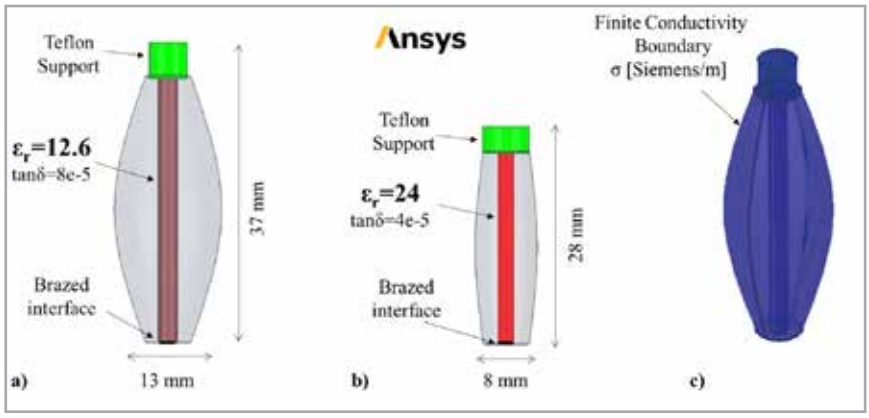

Fig. 2 - Proposed dielectric loaded combline resonator designed in Ansys HFSS: a) side view of resonator with ε_r=12.6, b) side view of resonator with ε_r=24, c) 3D view of resonator with background conditions of metallic cavity.

Two sixth-order elliptical filter models were designed using the dielectric loaded combline resonators in Fig. 2. The 3D models of proposed Ku-band filters are compared in Fig. 3 where the difference in size is highlighted.

Both filters are based on the same folded configuration in which all positive couplings between adjacent resonators are used while a negative cross-coupling has been designed between the non-adjacent resonators 2-5 to achieve two transmission zeros (TZs) in the lower and upper stop bands. The difference in footprint is shown in Fig. 4 where top views of the filters are presented.

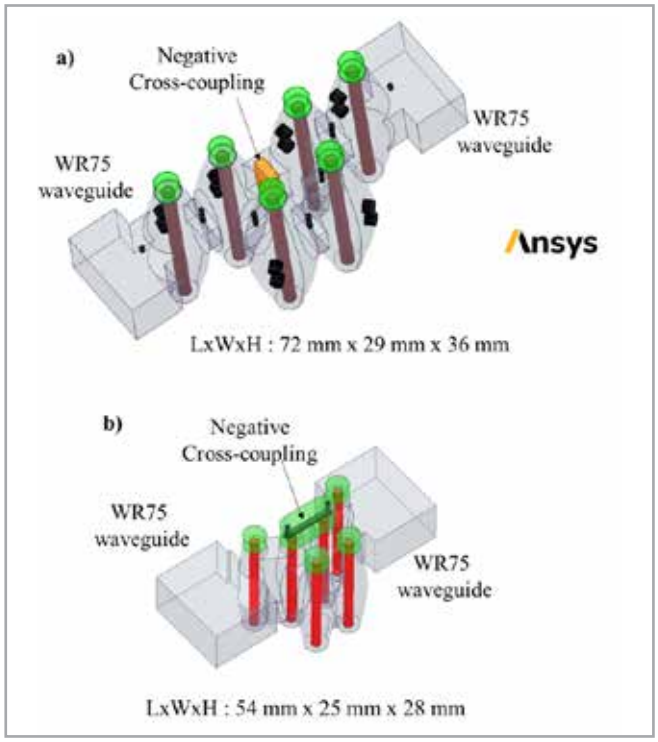

Fig. 3 - 3D view of sixth-order Ku-band filters: a) Model 1 (ε_r=12.6), b) Model 2 (ε_r=24).

The intra-couplings were designed by simulating odd and even resonant modes (eigenmode analysis) between each resonator duplet; whereas the Group Delay (GD) method was used to design the input couplings [9] where the WR75 waveguide interface was used. In this scenario, the GD of the reflection characteristic was simulated by performing a Driven Modal analysis of the S-parameters in HFSS. The models used to design the input and intra-couplings are shown in Figs. 5a and 5b, respectively, while Figs. 5c and 5d are the models used to design the negative cross-couplings.

In the first filter model in Fig. 3a, the negative cross-coupling was achieved by using a capacitive iris loaded with high-permittivity (ε_r=24) material [7]. This cross-coupling solution is impractical

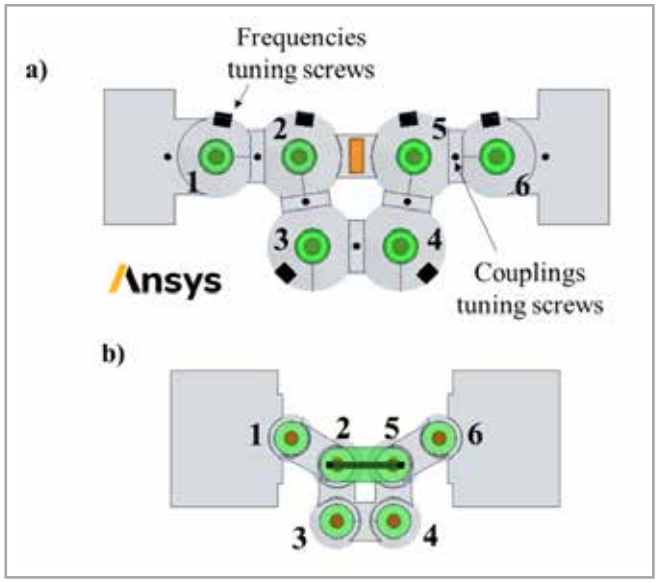

Fig. 4 - Top views of sixth-order Ku-band filters: a) Model 1 (ε_r=12.6), b) Model 2 (ε_r=24).

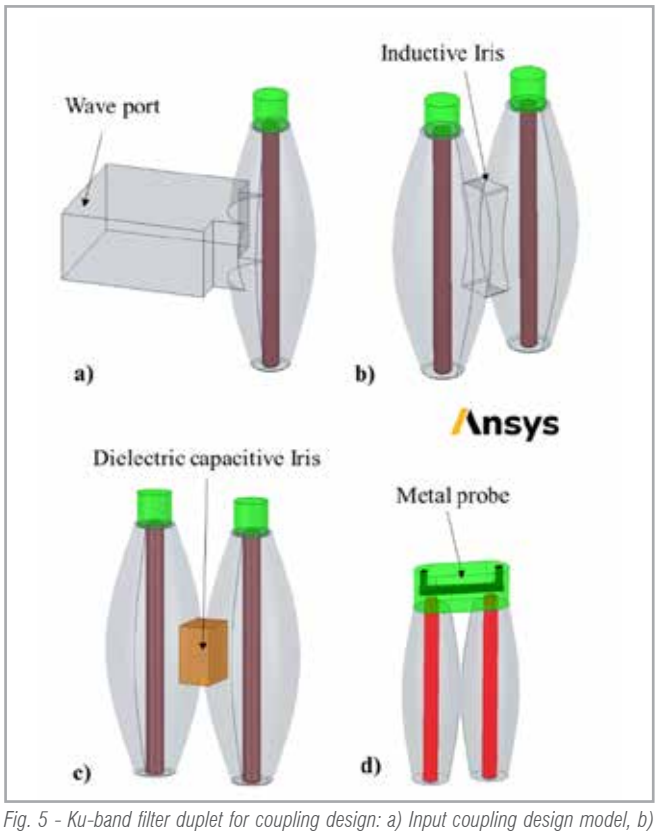

Fig. 5 - Ku-band filter duplet for coupling design: a) Input coupling design model, b) Intra-positive coupling design model, c) Negative cross-coupling design Model 1, d) Negative cross-coupling design Model 2.

in the second filter model because the smaller size of the structure does not allow the desired negative coupling value to be achieved. However, in this case the cross-coupling was achieved by designing a shaped metal probe supported by a Teflon interface (Fig. 5d).

In the first filter model (Fig. 3a), tuning screws were added to the cavity and coupling irises to compensate for the variation in filter response due to manufacturing tolerances. Similar tuning mechanisms can be used in the second filter model, however the structure shown in Fig. 3b is only a preliminary model, and the tuning screws are not present.

Simulated Results

Driven Modal simulations were performed in HFSS to simulate and optimize the S-parameters of both sixth-order Ku-band filters. In each case, the wave-ports were defined as signal excitations of the 3D model while the adaptive meshing solutions were used for the simulation setup. The central frequency of the filter (11 GHz) was chosen as the single solution frequency. Concerning the mesh, curvilinear elements were applied since the models show numerous curved surfaces. The full-wave response of the first sixth-order filter model (Fig. 3a) is shown in Fig. 6, while the simulated S-parameters of the second prototype (Fig. 3b) are depicted in Fig. 7. Both simulations converged with a maximum Delta-S magnitude of less than 0.01.

All in-band and out-of-band requirements (Fig. 6) are satisfied in the case of the first filter model. Return loss (RL) greater than 19 dB and insertion loss (IL) less than 0.8 dB are over the entire passband (240 MHz), while all near-band rejection requirements are met due

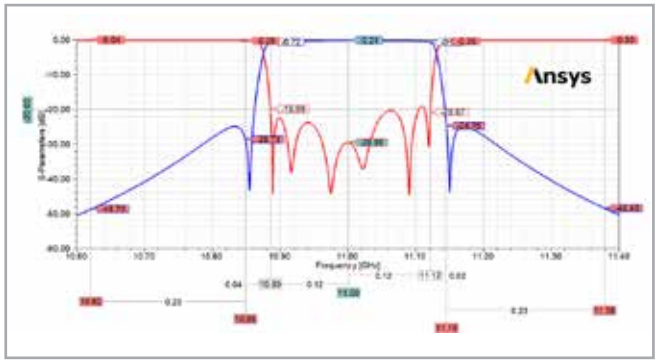

Fig. 6 - Simulated response of Ku-band filter Model 1 (blue line is transmission characteristic, red line is reflection characteristic).

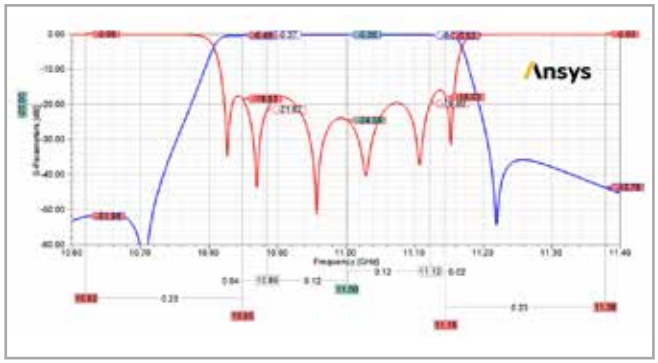

Fig. 7 - Simulated response of Ku-band filter Model 2 (blue line is transmission characteristic, red line is reflection characteristic).

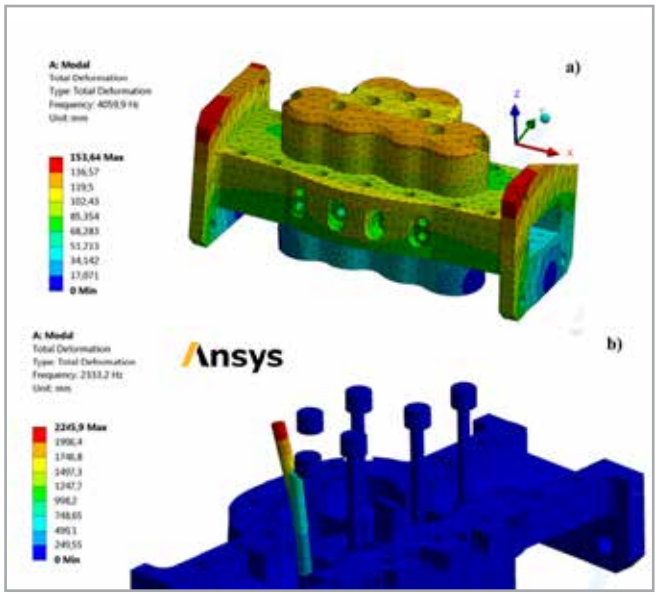

Fig. 8 - Ansys vibration analysis of the sixth-order filter Model 1.

to the TZs. Regarding the second filter model, similar results were obtained but a wider bandwidth was achieved despite using the higher permittivity values of the ceramic elements have been used. This shows that "strong" coupling values can be achieved with the proposed design even though the E-field is more confined within the dielectric elements.

The first model was chosen for manufacturing because it is less critical in terms of manufacturing tolerances, and therefore additional analyses were performed during the design procedure. Vibration analyses were performed in Ansys Mechanical to identify the first

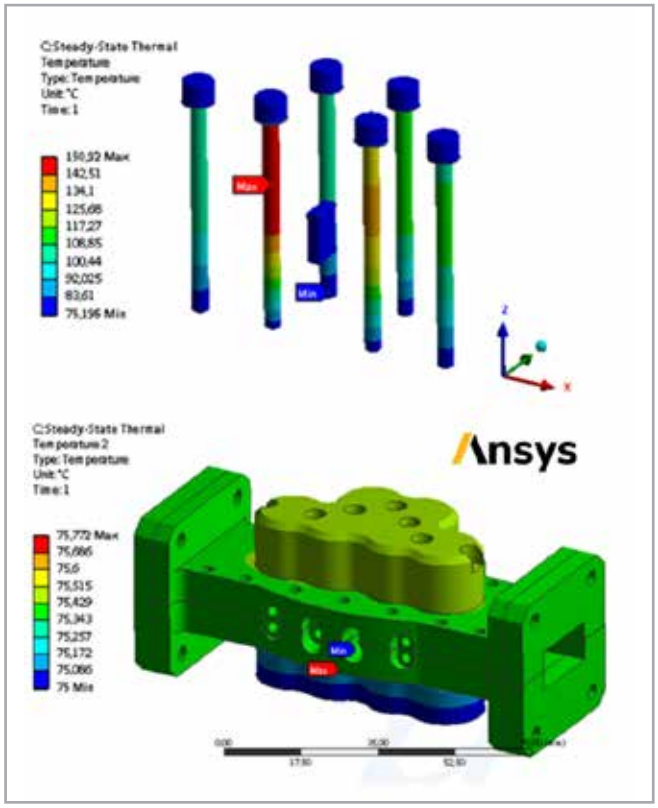

Fig. 9 - Ansys and HFSS high-power thermal simulations of the sixth-order filter Model 1 at the central frequency.

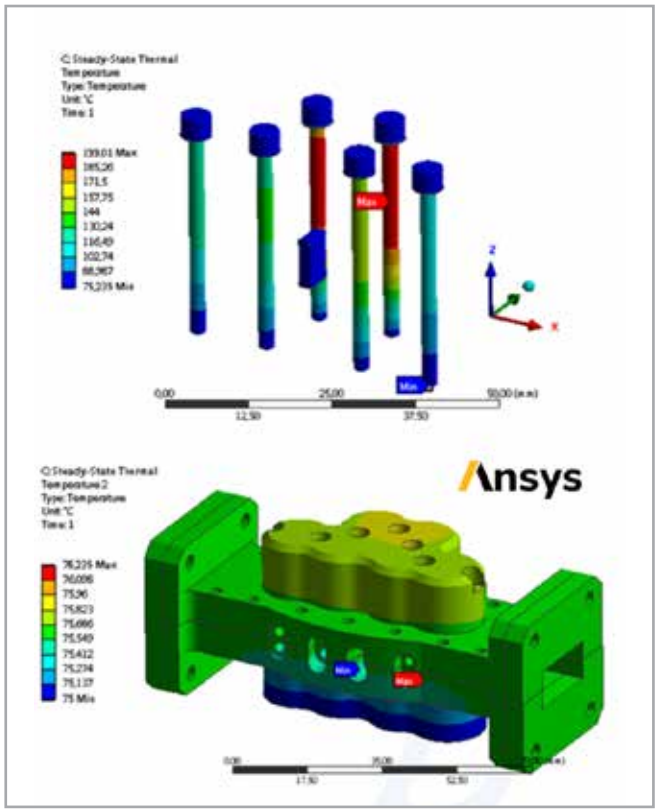

Fig. 10 - Ansys and HFSS high-power thermal simulation of the sixth-order Model 1 filter at the edge of the passband.

mechanical resonance mode of the sixth-order filter in Fig. 3a. As shown in Figs. 8a and 8b, the first modes are at 4059.9 Hz for the aluminum casing and at 2245.9 Hz for the ceramic cylinders, respectively; these are above the range of the specification for the vibration level (2000 Hz). Simulated results of the high-power thermal analyses performed at the central frequency are shown in Fig. 9.

A combination of HFSS and Mechanical simulations in Ansys Workbench was used to calculate the thermal drift with 150 W input power and to calculate the thermal drift of the S-parameter response. The simulations were performed including all physical properties of the metallic and dielectric parts. The estimated change in relative permittivity over the predicted temperature for the dielectric parts was also considered. A similar high-power thermal analysis was also performed at the passband edge frequency. The maximum temperature is reached on the ceramic elements, in particular the maximum temperature is 130 °C for the central frequency and 200 °C for the passband edge.

Concerning the thermal drift of the frequency, the maximum shift estimated by simulation is in the range 8÷16 MHz corresponding to 5÷8 ppm/°C (higher for the edge frequency, and lower for the central frequency). Fig. 10 shows the high-power thermal results of the analysis at the passband edge frequency.

High-power thermal simulations were also performed on the second filter model. However, the estimated temperature rise is greater due to the smaller volume and the smaller heat transfer surfaces. The maximum temperature reached on the ceramics is over 200°C.

Test Results

The first sixth-order Ku-band filter model was manufactured by achieving a volume reduction of about 50% compared to a standard filter based on the TE113 resonators, while keeping the Q-factor values compliant with the requirements. Fig. 11 shows the prototype of the manufactured filter and its 3D mechanical model, the structure is made of silver-plated aluminum. The final size (LxWxH) is 92mm x 45mm x 41mm with a mass of less than 200g in accordance with expectations.

The comparison between the measured (solid lines) and simulated (dashed lines) responses is shown in Fig. 12. According to [7], the measured response has shifted upward in frequency by about 100 MHz compared to the simulated response in Fig. 6. This is attributed to the actual value of the dielectric constant of the ceramic resonators that have a tolerance that is difficult to compensate for using only tuning screws. The actual value of the permittivity of the dielectric elements (ε_r=12.4) was used in the simulation for a proper comparison with the measurement as shown in Fig. 12.

The measured unloaded Q-factor is above 4500 as expected, and the out-of-band attenuation is very good taking into account the frequency shift. In addition, the insertion loss of less than 1 dB (objective) over the entire passband is compliant.

According to [8], the final environmental and high-power tests were also performed in this filter model and promising results were obtained. Fig. 13 shows the RF breakdown test setup in which the filter is placed inside the Thermal Vacuum Chamber (TVAC).

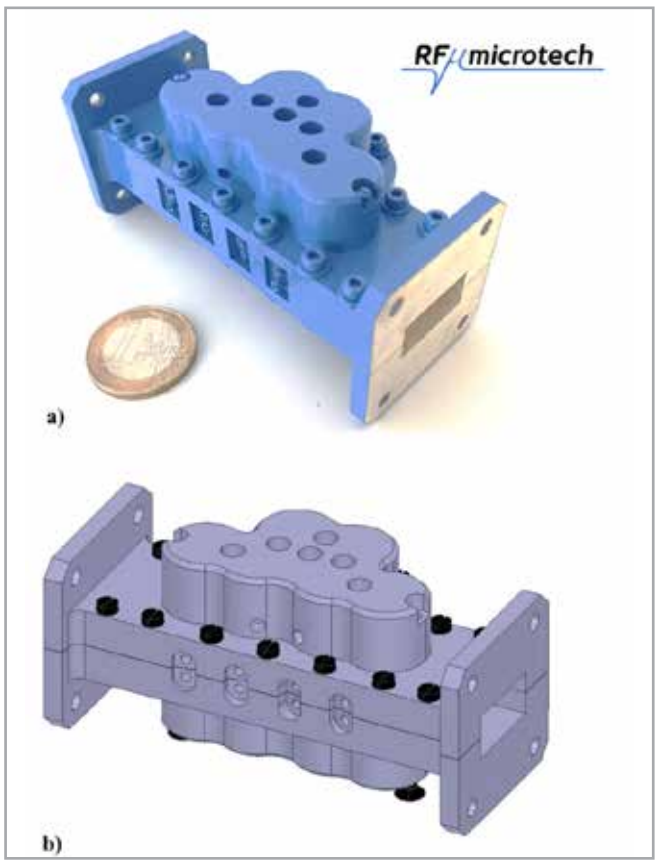

Fig. 11 - Manufactured (a) and mechanical (b) architectures of Ku-band filter Model 1.

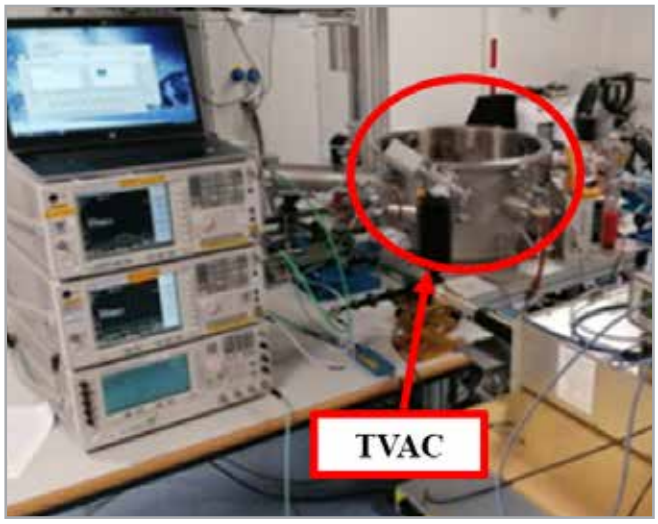

Fig. 13 - RF breakdown test setup.

Conclusions

Two compact sixth-order Ku-band elliptic filters for high-power satellite applications were designed as part of an ESA ARTES AT project in which compactness and power-handling in space environment are key requirements. In this paper, filters based on TM dielectric-loaded combline resonators combined with barrel-shaped cavities were presented in this paper and first experimental results are shown. Filter design and simulation were performed using Ansys software from both electronic and thermo-mechanical perspectives. In both filter cases, the geometries and materials were carefully chosen in order to improve the high-power performance in terms of power-handling and multipactor.

A first model was designed considering dielectric resonators with permittivity of 12.6 achieving volume and mass savings of about 50% compared to standard TE113 resonators. A second smaller prototype was proposed using ceramic elements with higher permittivity ($\varepsilon_r = 24$), however only a detailed analysis of the first model was performed and it was chosen for preliminary manufacturing and testing processes since it is less critical in term of manufacturing tolerances. In this scenario, the measured filter response of the first model shows promising results with an unloaded extrapolated Q-factor of about 4900.

According to preliminary test [8], multipactor discharges up to 1400 W at the central frequency were not obtained, while 130 W at continuous wave (CW) concerns the maximum power achieved from the power-handling point of view, which is slightly lower than the expected value (150 W). During the power-handling test, there was a non-negligible temperature rise in line with that predicted by thermo-mechanical simulations.

References

[1] R. V. Snyder, G. Macchiarella, S. Bastioli and C. Tomassoni, "Emerging Trends in Techniques and Technology as Applied to Filter Design", IEEE Journal of Microwaves, vol. 1, no. 1, pp. 317-344, winter 2021.

[2] R. V. Snyder, A. Mortazawi, I. Hunter, S. Bastioli, G. Macchiarella and K. Wu, "Present and Future Trends in Filters and Multiplexers", Microwave Theory and Techniques, IEEE Transactions, vol. 63, n. 10, 2015.

[3] X. Chi Wang and Kawthar A. Zaki, "Dielectric Resonators and Filters", IEEE Microwave Magazine, pp. 115-127, October 2007.

[4] M. Yu, "Power-handling capability for RF filters", IEEE Microwave Magazine, vol. 8, n. 5, pp. 1527-3342, 2007.

[5] L. Pelliccia, F. Cacciamani, A. Cazzorla, D. Tiradossi, P. Vallerotonda, R. Sorrentino, W. Steffè, F. Vitulli, E. Picchione, J. Galdeano, P. Martìn-Igleasis, "Compact On-board L-band Dielectric-loaded Diplexer for High-power Applications", 49th European Microwave Conference, EuMC, Paris, 2019

[6] S. Chi Wang, K. A. Zaki, A. E. Atia and T. G. Dolan, "Dielectric combline resonators and filters," in IEEE Transactions on Microwave Theory and Techniques, vol. 46, no. 12, pp. 2501-2506, Dec. 1998, doi: 10.1109/22.739240.

[7] P. Vallerotonda, F. Cacciamani, L. Pelliccia et al., "Dielectric-loaded Ku-Band Filter for High-power Space Applications based on Barrel-shaped cavities". Accepted for European Microwave Week Conference (EuMW), London, February 2022.

[8] P. Vallerotonda, F. Cacciamani, L. Pelliccia et al., "Ceramic-loaded Barrel-shaped Ku-band filter for High-power Satellite Applications". Accepted for International Microwave Filter Workshop (IMFW), Perugia, Italy, November 2021.

[9] Richard J. Cameron, Chandra M. Kudsia and Raafat R. Mansour, "Microwave Filters for Communication Systems," 2007.

Acknowledgment

The filters described in this paper are the outcome of the ESA ARTES AT project named DOMUK (ESA Contract Number: 4000125645/19/NL/NR). We would like to thank the staff of ESA ESTEC (in Noordwijk, The Netherlands), ESA-VSC Lab (in Valencia, Spain) and the University of Perugia (in Perugia, Italy) for their contributions and support.

This work is dedicated to the memory of Prof. Roberto Sorrentino, whose work, honesty, and integrity will forever inspire his past students and colleagues towards excellence.